View metadata, citation and similar papers at core.ac.uk
brought to you by CORE
provided by Repository@USM

CHARACTERISATION OF SOLID WOOD AND ALMOND GUM BONDED *Rhizophora spp*. PARTICLEBOARD AS BREAST PHANTOM FOR MRI AND CT

BAKER (M. TAYSEER) ABDALLAH ABABNEH

UNIVERSITI SAINS MALAYSIA

2016

CHARACTERISATION OF SOLID WOOD AND ALMOND GUM BONDED *Rhizophora spp*. PARTICLEBOARD AS BREAST PHANTOM FOR MRI AND CT

by

BAKER (M. TAYSEER) ABDALLAH ABABNEH

Thesis submitted in fulfillment of the requirements
for the degree of
Doctor of Philosophy

September 2016

ACKNOWLEDGEMENT

The submission of this thesis gives me an opportunity to express all praises to Allah, the Almighty, Merciful and Passionate, for granting me the strengths to complete this work.

I highly show my regards to my main supervisor Dato' Prof. Dr. Abd Aziz bin Tajuddin for his great support, guidance in completion of my research work and patiently correcting my writing. I attribute the level of my PhD degree to his great help and encouragement. One simply could not wish for a better or friendlier supervisor.

I would also like to express my great thanks to my co-supervisor, Prof. Dr. Rokiah Hashim, for her excellent guidance, caring, patience, and providing me with an excellent atmosphere for doing my research. She is really very expert in her field and has directed me through various situations, allowing me to reach this accomplishment. To her, I am eternally grateful.

Besides, I would like to thank my second co-supervisor, Prof. Dr. Ibrahim Lutfi Shuaib for the continuous support of my PhD study and research. His guidance and insightful comments and suggestions helped me in all the time of research and writing of this thesis.

Special thanks go to the supporting staff of the laboratories in School of Physics, School of Industrial Technology, and Advanced Medical and Dental Institute (AMDI) who helped me in many different ways to conduct the experiments in a specific manner.

I am also grateful to the people who helped and contribute great ideas and advices, especially my close friends: Dr. Ali Abuarra, Dr. Amer Aljarah, Dr. Ehsan

Tousi, Dr. Mohamad Wasef, Mrs. Suzana Mat Isa, and Mr. Rizal. Without them, this study would not be possible.

Special thanks go to my parents, brothers and sisters, who have been the pillars behind the completion of my research by giving moral support and prayers. This work would never have been the light of the day: had it not been for my parents. I am profoundly grateful to them.

Finally, I offer my regards and blessings to all of those who supported me in any respect during the completion of the research, as well as expressing my apology that I could not mention personally one by one.

TABLE OF CONTENTS

LIST OF TABLES

Page

LIST OF FIGURES

Page

LIST OF ABBREVIATIONS AND SYMBOLS

α	Alpha
β	Beta
γ	Gamma
μ	linear attenuation coefficients
μ/ρ	Mass Attenuation Coefficient
μ_w	linear attenuation coefficients of water
ρ	Density
ρ_e	Electron density
ω_0	Precession Frequency
a_i	Electrons fraction
w_i	Weight fraction
1D	One dimension
2D	Two dimensions
A	Ampere
Al	Aluminium
AL	Almond Gum
B_0	Strength of the External Magnetic Field
B_1	Variable Magnetic Field
B_{osc}	Oscillating Field
CHNS	Carbon Hydrogen Nitrogen Sulfur
Co-60	Cobalt-60
Cs-137	Caesium-137
CSF	Cerebrospinal fluid
CT	Computed Tomography
eV	Electron volt
FE-SEM	Field emission-scanning electron microscopy
FSE	Fast Spin Echo
FTIR	Fourier Transform Infrared
GE	General Electric
GRE	Gradient Echo
HU	Hounsfield Units

Hz	Hertz
į	Unit vector along the x axis
I	Intensity of attenuated narrow beam of gamma-ray
I_0	Intensity of un-attenuated narrow beam of gamma-ray
IB	Internal Bond
JIS	Japanese Industrial Standards
KBr	Potassium bromide
kVp	Peak kilovoltage
LEGe	Low Energy Germanium
m/v	Mass by Volume
M_0	Initial Net Magnetization
MC	Moisture Content
MF	Melamine Formaldehyde
MOE	Modulus of Elasticity
MOR	Modulus of Rupture
MRI	Magnetic Resonances Image
MXY	Magnetization Along XY axis
Mz	Magnetization Along Z axis
N/mm^2	Newton per square millimetre
NMR	Nuclear Magnetic Resonance
^oC	Degree Celsius
PF	Phenol formaldehyde
PIU	Percent integral uniformity
QA	Quality accuracy
QC	Quality control
RF	Radiofrequency
ROI	Region of interest
SE	Spin- Echo
SNR	Signal noise ratio
spp	Species
SD	Standard Deviation
T	Tesla

t	Time
T1	Longitudinal Relaxation
T2	Transverse Relaxation
TE	Echo Time
TR	Repetition Time
Ts	Thickness swelling
UF	Urea formaldehyde
UTE	Ultrashort TE
V	Volt
w/w	Weight by weight
WA	Water Absorption
w_c	Angular Velocities
XCOM	X-ray computed
XRF	X-ray fluorescence
Z	Atomic number
Zeff	Effective atomic number

PENCIRIAN *Rhizophora spp*. KAYU PADU DAN PAPAN PARTIKEL BERIKAT GUM ALMOND SEBAGAI FANTOM PAYUDARA UNTUK MRI DAN CT

ABSTRAK

Tujuan penyelidikan ini adalah mengkaji kesesuaian penggunaan keaslian (kayu padu asli) fabrikasi *Rhizophora* spp. Papan partikel sebagai fantom payu dara bagi penggunaan aplikasi MRT dan CT. Masa santaian T1 dan T2, nombor-nombor CT dan ketumpatan bagi *Rhizophora* spp. padu, dengan tiga peratus kandungan MC yang mempunyai kelembapan yang berbeza (33%, 24% dan 16%) ditentukan masing – masing melalui penggunaan imbasan MRI dan CT, untuk digunakan sebagai fantom yang sesuai bagi payu dara. Hal ini kerana ia mempunyai masa santaian yang sama seperti tisu lembut payu dara. Masa santaian 33% dan 24% amat dekat dengan nilai tisu lembut, terutamanya tisu payu dara. Di samping itu, nombor CT dan ketumpatan sampel juga berada dalam julat yang sama dengan tisu lembut. Seterusnya, papan partikel almond gum (AL) terikat *Rhizophora* spp. difabrik dengan tiga partikel saiz (425 - 210 µm, 210 - 74 µm, dan< 74 µm) pada tiga tahap perekat AL yang berbeza (0%, 8%, dan 16%), untuk menentukan sama ada ia sesuai digunakan sebagai fantom payu melalui aplikasi MRI dan CT. Nombor CT, kepadatan, mekanikal dan ciri-ciri fizikal, sifat pengecilan menunjukkan bahawa sampel papan partikel merupakan fabrikasi fantom payudara yang sesuai. Berdasarkan keputusan kajian, penggunaan almond gum sebagai bio perekat terikat *Rhizophora spp*. masa zarah menunjukkan suatu penambahbaikan dalam ciri-ciri fizikal dan mekanikal. Bagi sifat pengecilan, ia ditemui bahawa fabrikasi papan menghampiri nilai tisu (Payudara 1) yang dikira melalui program komputer XCOM. Sampel papan partikel dengan sifat optimum yang digunakan bagi fabrikasi fantom

payudara separa bulat dengan saiz 16 × 8 × 8 cm (L × H × T). Perspeks fantom payu dara juga digunakan dalam kajian inidengan saiz dan bentuk yang sama seperti fantom papan partikel. Imbasan MRI dan CT merupakan hubungan yang baik diantara data bagi fantom payu dara papan partikel *Rhizophora spp*. yang difabrik dengan data bagi fantom perspeks, dimana nombor CT berjulat daripada - 6.29 hingga 28.57 HU dan 102.43 hingga 116 HU, dan kepadatan masing-masing 1.03g/cm^3, 1.14g/cm^3. Nilai keseragaman untuk dua fantom terpilih termasuk dalam had kategori ≤ 5 HU, iaitu 4.32 HU dan juga 1.07 HU, bunyi oleh fantom payu dara papan partikel *Rhizophora spp*.dan fantom perspeks payu dara adalah masing-masing sebanyak 4.91 dan 2.71. Empat tiub air dalam fantom yang dirangsang dapat dilihat dengan jelas dan terdapat dalam imej MRI dan CT kedua-dua fantom payu dara. Dua daripada fantom payu dara difabrik wujud dengan taburan skala kelabu yang sama dalam imej CT, yang menunjukkan ketumpatan yang seragam dan komposisi yang sekata.Nilai kuantiti daripada pengukuran imej MRI adalah nilai-p untuk fantom payu dara papan partikel diantara T1 dan T2 keberatan imej yang didapatai adalah sebanyak 0.066 tidak signifikan dan bersamaan 0.232 signifikan bagi fantom perspek payu dara. Begitu juga, nilai kedua-dua fantom mencapai nilai yang diperlukan harus kurang daripada atau sama dengan 0.025. Berdasarkan keputusan di atas, papan partikel almond gum (AL) terikat *Rhizophora spp*. dapat dicadangkan sebagai bahan yang sama untuk tisu fantom dalam aplikasi CT dan boleh dianggap tetingkap baru terbuka untuk melakukan lebih banyak kajian yang dapat digunakan sebagai rujukan dalam fantom MRI dan radiologi yang lain.

CHARACTERISATION OF SOLID WOOD AND ALMOND GUM BONDED *Rhizophora spp*. PARTICLEBOARD AS BREAST PHANTOM FOR MRI AND CT

ABSTRACT

The aim of this research is to study the suitability of using natural (fresh solid wood) and fabricated *Rhizophora* spp. particleboard as a breast phantom for MRI and CT application. The relaxation times T1 and T2, CT numbers and density for the fresh *Rhizophora* spp., with three different MC percentages (33%, 24% and 16%) were determined using an MRI and CT scan respectively, to be a suitable phantom for a breast, as they have similar relaxation time to soft tissue of the breast. The relaxation times of 33% and 24% were very close to the soft tissue value, particularly breast tissue. In addition, the CT numbers and density of samples in the same range of soft tissue. Then, almond gum bonded *Rhizophora* spp. particleboard were fabricated with three particle sizes (425 - 210 µm, 210 - 74 µm, and < 74 µm) at three different almond gum adhesive levels of 0%, 8%, and 16%, to see if they could be used as a suitable breast phantom via an MRI and CT application. The CT numbers, density, mechanical and physical properties, characterization and attenuation properties were found to indicate what particleboard samples are most suitable to fabricate breast phantoms. Based on, the results of this study, using almond gum as a bio adhesive bonded with *Rhizophora* spp. particleboard achieves a noticeable improvement in the physical and mechanical characteristics. For attenuation properties, it was found that the particleboard fabrication close from the water and young - age (Breast 1) tissue calculated value by XCOM computer program. The particleboard samples with the optimum properties were used for the fabrication of a semicircular breast phantom with a size of 16 × 8 × 8 cm (L × H ×

T). Perspex breast phantoms were also used in this study with the same size and shape as the particleboard phantom. The MRI and CT scan indicated good agreement between the data of the fabricated *Rhizophora* spp. particleboard and that of the Perspex breast phantom, where the CT numbers range from -6.29 to 28.57 HU and 102.43 to 116 HU, and the density 1.03g/cm^3, 1.14g/cm^3, respectively. The uniformity values for two selected phantoms fall within the advised limit of $\leq$ 5 HU, which 4.32 HU and 1.07 HU also, the noise of *Rhizophora* spp. particleboard and Perspex breast phantoms are 4.91 and 2.71 respectively. The 4 tubes water inside the simulated phantoms were clearly seen and precisely localized in the MRI and CT images of the two breast phantoms. Two of fabricated breast phantoms appeared with similar grayscale distribution in the CT images, which indicated the uniform density and homogenous composition. The quantification value from the MRI image measurements, were the p - value measurement for particleboard breast phantoms between T1 and T2 weighted image it found 0.066 non significant and equal 0.232 significant for Perspex breast phantom. Also, the ghosting values of two phantoms achieved the required value should be less than or equal to 0.025. Based on the above results, *Rhizophora* spp. particleboard bonded almond gum can be highly recommended as a material of tissue equivalent phantom for CT applications and can be considered open new window to doing more study to be possible for use as a reference in MRI phantoms and other radiological areas.

CHAPTER ONE: INTRODUCTION

1.1 Introduction

Phantoms are composed of tissue-mimicking materials, with the majority of phantoms having a simple homogeneous internal structure. Simple or complex targets are sometimes embedded within phantoms to mimic internal structures or to serve as characterization targets. Tissue mimicking materials must exhibit properties of the human body such as, mass density and electron density, relaxation times or speed of sound.

Phantoms and anthropomorphic phantoms are available commercially, mimicking many tissue organs and organ systems. Commercial phantoms range in price from hundreds to thousands of us dollars and are often preferred for training and calibration of imaging devices. However, commercial phantoms are typically designed for broad markets and specific applications, and are not customizable. For this reason, customized design and fabrication of tissue phantoms are required for more specialized applications requiring tailored properties or dimensions, or when seeking to reduce cost. A water phantom is considered the primary dosimetry phantom recommended because water is a perfect match with the soft tissue. However, it is not always practical to perform dosimetry measurements in a liquid medium, so a solid homogeneous phantom based on polystyrene, acrylic and other proprietary materials has become the preferred substitute for water phantom (Khan, 2010).

Material tissue equivalents are widely used in routine quality assurance (QA) and quality control (QC) for the diagnostic and therapeutic physics. In radiotherapy, they are generally used for computed tomography (CT) calibration number in

treatment planning systems. Magnetic resonance imaging (MRI) phantoms are useful for calibration and verification of imaging equipment, the development of new systems and pulse sequences, and training for MRI operators. Moreover, they are often using the phantom measure the doses delivered to patients undergoing various therapeutic procedures.

In recent years, interest in research related to the interactions of electromagnetic radiations with biological tissues has continuously increased. Such situations present in the case of medical imaging and ultrasound therapy, magnetic resonance imaging and computed tomography procedures; therefore, there is a high demand for materials that can mimic particular human tissue properties and which can be used to build test phantoms.

There are some species of wood and natural materials that have been studied and qualified as water equivalent materials and the human body for the fabrication phantom for ionizing radiations, (Bradley et al., 1991). It reported for the first time that some tropical hardwoods have linear attenuation coefficients including *Rhizophora spp*. as equivalent materials with mass density equivalent. There are many researchers who have focused on the suitability of the mangrove hardwood *Rhizophora spp*. as tissue equivalent phantom material. For examples Tajuddin et al. (1996), Bauk and Tajuddin (2008), Shakreet et al. (2009), Abu Arra et al. (2014) and others references shown in the next chapter.

Rhizophora spp. is one of genera most abundant from tropical mangrove trees (Alias et al., 2010). There are many species of *Rhizophora* trees such as *Rhizophora mucronata, Rhizophora harrlsonii, Rhizophora stylosa, Rhizophora mangle,* and others (Tomlinson, 1986). However, *Rhizophora* spp. means all species

of *Rhizophora*. Specifically, *Rhizophora* spp. could be used as a phantom in two general forms:

1- Solid raw wood: No treatment and in addition to other materials.

2- Particleboard: Defined as a wood-based composite that consists of cellulosic particles of different shapes and sizes bonded together with a binder under heat and pressure (JIS, 2003).

Particleboard can also be manufactured without the use of any adhesive, which is called binderless particleboard. The connection is due to the presence of free sugars and lignocellulosic materials in the timber tissues where heat and pressure would make the binders in the particleboard. However, binderless particleboard has mass attenuation coefficient properties that are preferable and it also has a lower internal bond strength and dimensional stability in the case of water absorption and thickness swelling (Marashdeh, 2013)

In general, there are two types of adhesive firstly, synthetic adhesive (chemically manufactured adhesive) and the second type is bio – based adhesive. Formaldehyde-based adhesives have been the most widely used in the wood industry (Rokiah et al., 2009). There are many studies on *Rhizophora spp*. particleboards using the synthetic adhesive such as studies by Surani (2008) and Ngu (2009) with different particle size, different levels adhesive treatment and different densities of particleboard production targets. When the mass attenuation coefficient of *Rhizophora spp*. particleboard with the synthetic adhesive is significantly far from the breast tissue and water, it has improved the internal bond strength and dimensional stability of the panels. At same time, serious gaseous emissions are created that are harmful to humans and the environment, which are considered a

synthetic adhesive that is a carcinogenesis substance by the International Agency for Research on cancer (IARC) (Bosetti et al., 2008; Rokiah et al., 2009).

Therefore, to solve this problem it was suggested to use a bio-based adhesive from a natural source which is considered the second type of adhesive (Tousi et al., 2014b). It has the following advantages: stronger, safer and cheaper compared with synthetic adhesives.

Several fruit-bearing trees belonging to the rosaceae family, such as peach (*Prunus persica*), damson (*Prunus insitia*), egg plum (*Prunus domestica*), cherry (*Prunus cerasus* and *Prunus virginiana*) and almond (*Prunus dulcis*), can produce abundant amounts of gum exudates from the trunk (Rahimi et al., 2013), as a consequence of a disease (gummosis) and/or a mechanical injury followed by a microbial attack (Mahfoudhi et al., 2012). In particular, gum exudates from the trunk of the almond trees (*P. dulcis*) represent a potential natural resource of hydrocolloid gums. almond gum can be found in different shapes, sizes, and colors (white, light yellow, amber, red, and/or brown), which are widely available in the Middle East as well as throughout Mediterranean Africa. The chemical composition of the almond gum was determined (Mahfoudhi et al., 2012), showing that high amount of carbohydrates and protein as well as a low fat content are present. Exudates are also relatively rich in minerals, in particular, potassium, magnesium and calcium. Almond gum can potentially be used in foods, pharmaceuticals, and other industries. In recent years, it is being used as a suspending or emulsifying agent in combination with Arabic gum and gum tragacanth in pharmacy, edible gels and pastilles, stabilisation of milk–orange juice mixtures, colours, clothing (for stiffness of clothes), and isolating the surface of boats (Rahimi et al., 2013).

In the present study, *Rhizophora spp.* particleboard bonded with almond gum (AL) is used for fabricate of tissue, the equivalent phantom material for magnetic resonance imaging (MRI) and computed tomography (CT) applications.

Firstly, measurements of the density, PH characterization, viscosity properties, thermal properties, Fourier transform infrared (FTIR) spectrometer characterization, carbon hydrogen, nitrogen and sulfur (CHNS) chemical compositions, microstructure analysis by field emission scanning electron microscope (FE-SEM), and the linear and mass attenuation coefficients of the almond gum based *Rhizophora spp.* particleboards at effective energy range from 16.60 to 25.30 keV using X-ray fluorescent (XRF).

Secondly, the effects of *Rhizophora spp*. particle size and almond gum (AL) percentage of the fabrication particleboard on the physical, mechanical, and structural properties were studied. Three different particles sizes ($\leq$ 74µm, 74 µm–210 µm, and 210 µm–425 µm) of *Rhizophora spp*. bonded with three almond gum (AL) percentage levels (0%, 8%, and 16%) were used. However, the terms of moisture content (MC) were investigated, along with density, internal bond (IB) strength, modulus of rupture (MOR), thickness swelling (TS), water absorption (WA), chemical composition used carbon hydrogen, nitrogen and sulfur (CHNS) analysis, and microstructure analysis, using scanning electron microscopy and energy dispersive X-ray (SEM/EDX) spectroscopy. In addition, measurements were made of the liner and mass attenuation coefficients via the use of X-ray fluorescent (XRF) at photon energies ranging from 16.6–25.3 keV. This was done by studying the attenuation of X-ray fluorescent (XRF) photons from niobium, molybdenum, palladium, silver and tin targets at K_α peaks. The results were compared with

theoretical values for average breast tissue for young – age, and water calculated by using XCOM computer code (Berger and Hubbell, 1987).

Finally, magnetic resonance imaging (MRI) was used to study the relaxation time and computed tomography (CT) scan used to study the density distribution profile, of the fabricated particleboards and fresh wood with different moisture contents (MC). These were done to obtain the most suitable samples to fabricate breast phantom to use in MRI and CT applications.

1.2 Problem Statement

The phantom is defined as a mass of solid or liquid media, which is designed to simulate the ionizing radiation attenuation properties of the human body (Attix, 2008). There are various commercial phantoms that were created to study the quality control (QC) tests and calibrations and to compare the performance of an imaging system in the medical field (O'Connor, 1999). However, these commercial phantoms are considered laborious, expensive, and sometimes, not available in some institutions due to financial limitations, and there must be specific shapes and sizes according to the experiment required (Khan, 2010). With such a variety of imaging technologies available, for example, magnetic resonance imaging (MRI) and computed tomography (CT), each of them has their own unique advantages and disadvantages. The ability to perform comparisons is critical in determining the optimal imaging parameters and clinical utility of each modality. The ideal platform for comparisons would be a well- characterized phantom that can be used to evaluate the ability to mimic image contrast, and tissue structure across all of the available modalities. An image is produced via two different mechanisms in MRI and CT imaging, which are characterized by different inherent tissue properties: T1 and T2 relaxation times for MRI and attenuation coefficients for a CT scan. Therefore,

phantom materials must simultaneously mimic both of these inherent tissue properties. In addition, it is important that the phantom mimics the complex structure between fibroglandular and adipose tissues present in the human breast, and it is useful in a diagnosis image. In this study fabrication of a new phantom is presented, based on *Rhizophora spp.* wood, which is useful in MRI and CT.

While fabricated *Rhizophora spp.* was studied by other researchers as noted in the literature review, the study on *Rhizophora spp.* binderless particleboard showed good agreement in dosimetric properties and with other standard phantom materials in ionizing radiation dosimetry. However, it is not in agreement with mechanical properties especially in dimensional stability (Marashdeh, 2013). In addition, using synthetic binders should be avoided because of the harmful emissions as mentioned earlier.

For these reasons, a phantom has been fabricated as a new tissue equivalent breast phantom that has the mechanical and physical properties, is environmentally friendly, cheap, and easy to use in MRI and CT. Almond gum is used as a bio-adhesive bonded with *Rhizophora spp.* particleboard, where until now there has been no information about the use of almond gum as an adhesive. This will be the first study of its kind using almond gum bonded with *Rhizophora spp*. particleboards. Moreover, this study will design and fabricate *Rhizophora spp*. as humanoid breast phantom, considering this research as the primary work in the field of medical physics in terms of using a non - ionizing radiation from an MRI device to study the characteristics of *Rhizophora spp*. phantom and to get the appropriate phantom for a female breast.

1.3 Significance of research

The significance of this research is the phantom fabrication from *Rhizophora spp*. wood for used in MRIs and CTs, which would open a new field on investigating the *Rhizophora spp*. wood properties by MRI, process that have the same T1 and T2 relaxation times as well as those similar of a human breast tissue. This work will also investigate the efficacy of utilizing almond gum (AL) bonded *Rhizophora spp*. particleboard which is cheap, non-chemical based, and fabricated from local material to reduce the cost of purchasing commercial ones.

1.4 Objectives of Research

The overall objective of this study is to design, and fabricate a new phantom from *Rhizophora* spp. wood to be tested using MRI and CT facilities, with a focus on MRI properties as equivalent materials for the human breast. Here a few minor objectives to achieve the main objective:

1- To design, fabricate and evaluate the concentrations of the different chemical components, physical and mechanical properties, and mass attenuation coefficient of *Rhizophora spp.* particleboard samples.

2- To characterize the almond gum bonded *Rhizophora* spp. particleboard and *Rhizophora* spp. fresh wood as tissue equivalent breast phantom using MRI and CT scan techniques.

3- To evaluate the effect of moisture content of *Rhizophora spp*. fresh wood as tissue equivalent breast phantom for MRI and CT scan.

4- To fabricate a phantom from a *Rhizophora spp.* sample most stability as tissue equivalent to manufacturing breast phantom size of 16 cm × 8 cm × 8 cm to use in MRI and CT scans.

5- To study the performance of two types of breast phantoms in MRI and CT scans and compare their results since the phantoms are critically important for the development of innovative diagnostics imaging techniques.

1.5 Scope of Research

This research would introduce two type from of the mangrove *Rhizophora* spp. wood (solid wood, fabricated particleboards bonded almond gum), which are equivalent to human tissues with appropriate relaxation times and CT numbers will be utilized in the design of a breast phantom for MRI/CT imaging. As well as, attenuation properties, characterization will be investigated. A quantification values will be inserted into this phantom to evaluate the performance of the MRI / CT scan value. The fabricated particleboard phantom will be evaluated in comparison with standard Perspex breast phantom.

1.6 Thesis Organization

This thesis includes five chapters, starting with the introduction in Chapter 1, where the utilization of tissue equivalent materials for phantom fabrication will be presented. It also gives a brief description of *Rhizophora spp.* fresh wood, particleboards, almond gum (AL), MRI and CT scans in addition to the study problem, significance of research, objectives of research, and thesis organization.

Chapter 2 contains the theoretical background, followed by a literature review relevant to this study, which describes the basic principles of the magnetic resonance imaging (MRI), computed tomography (CT) scans, and XRF technique.

Chapter 3 discusses the materials and methods of the preparation of materials and the fabrication of the particleboard samples preparation, and testing the physical, chemical, mechanical microstructure properties of the *Rhizophora spp.* and almond

gum. In addition, the method for evaluating the relaxation times and CT numbers of the samples will be discussed. Next, the fabrication of the breast phantom will be discussed determine the quantification values of MRI and CT scans.

Chapter 4 focuses on the results and discussions of all experiments performed in this study: the physical, mechanical, chemical and microstructure testing of the *Rhizophora spp*. fresh wood, almond gum, almond gum based *Rhizophora spp.* particleboard, also the relaxation times (T1, T2), CT numbers, determination of the density of the samples, attenuation coefficients of the samples and theoretically calculated value of water and young age breast tissue. Then, the quantification values of MRI and CT scans for breast phantom fabricated particleboard phantom are compared with Perspex standard phantom. Finally, in Chapter 5 precedes the conclusions and gives recommendations for future works.

CHAPTER TWO: LITERATURE REVIEW

2.1 Magnetic Resonance Imaging (MRI)

2.1.1 Basic Principle and History of MRI

Before beginning a study of the science of MRI, it will be helpful to reflect on the brief history of MRI.

In 1952, Bloch and Purcell were awarded the Nobel Prize in physics for discovered the magnetic resonance phenomenon independently in 1946. In the period between 1950 and 1970, NMR was developed and could be used for chemical and physical molecular analysis on liquids and solids (Purcell, Torrey, & Pound, 1946). Then in 1971 Raymond Damadian discovered that hydrogen signal in cancerous tissue is different from that of healthy tissue because tumors contain more water. More water means more hydrogen atoms. That showed the nuclear magnetic relaxation times of tissues and tumors differed motivating scientists to use MRI to study disease (Damadian, 1971). The first human being MRI examination did not occur until 1977, with the advent of computer techniques that develop images from MRI information. Edelstein and coworkers demonstrated imaging of the body using Ernst's technique in 1980. In 1986 Le Bihan publishes an article in Radiology, which describes diffusion weighted imaging (DWI) (Le Bihan et al., 1986). A single image could be acquired in approximately five minutes by this technique. By 1986, the imaging time was reduced to about five seconds, without sacrificing too much image quality (Hornak, 2008). In 1991, Richard Ernst was rewarded for his achievements in pulsed Fourier Transform NMR and MRI with the Nobel Prize in Chemistry. Many scientists over the next 25 years developed MRI into the technology that we now know today.

Magnetic resonance imaging (MRI) is derived from nuclear magnetic resonance (NMR). Hence the properties of the nucleus in the magnetic field are of most importance. Nuclei used in MRI are proton (1H), carbon (13C), and phosphorus (31P). The nuclei must have non-homogenous charge distributions. All fundamental particles possess a property called spin, which can be explained as a rotation of the nucleus around its own axis. Due to spin and the non-homogenous charge distribution (i.e. a moving charge), the nucleus produces a magnetic moment. MRI signal depends on the number of nuclei and their magnetic moments. Clinical MRI uses the magnetic properties of the nuclei and their interactions with large external magnetic fields and radiowaves to produce high spatial resolution MRI images. Hydrogen is the best choice of the MR active nuclei because of its high abundance in the human body and its high magnetic moment compared to other nuclei (Hendee and Ritenour, 2003), which means that the nuclei have characteristics prompting their tendency to align their axis of rotation when the magnetic field is applied to them. Total magnetic moment of the nucleus refers to the physical property responsible for such an alignment. From the law of quantum mechanics, the magnetic moment is only present in odd numbers of protons in the nuclei. With this, the nuclei can only interact with the magnetic field applied to them. The strength of the total magnetic moment is different for different nuclei and can determine its sensitivity towards magnetic resonance (Westbrook and Roth, 2011).

2.1.1(a) **Nuclear Spin and Behavior in Magnetic Field**

Electromagnetism tells us that a current carrying conductor, e.g. a piece of wire, produces a magnetic field encircling it. When the wire is formed into a loop, the field acts perpendicular to the surface area of the loop. Analogous to this concept is the field produced by negatively charged electrons orbiting the nucleus in an atom, or the spinning charges of the nucleus itself. This spinning momentum of nuclear charges is called "spin". Spin is a fundamental property of nature, like an electrical charge or mass. Spin comes in multiples of 1/2 and can be + or –, which produces a small magnetic field referred to as a magnetic moment (Burstein and Gray, 2003; Hornak, 2008).

When the nuclei are placed in an external magnetic field, behaves like a small magnetic bar, e.g. a patient placed in a MRI scanner. They begin to align almost parallel to the direction of the field (i.e. the same way a compass aligns to the magnetic field of the earth) due to spin and the laws of quantum mechanics. In the case of the hydrogen nucleus with a single proton at a spin quantum number, I=1/2, the proton does not align perfectly to the field. Due to the torque it experienced from the magnetic field, it will precess around the field's direction (Brown et al., 1998) as shown in Figure 2.1. The frequency of precession (known as the Larmor frequency) can be derived from both classical and quantum mechanics. The Larmor equation is given in Equation 2.1, where ω_0 is the precession frequency, γ is the gyromagnetic ratio and B_0 is the strength of the external magnetic field. For the proton, in field strength of 1.5 T, this frequency is about 63.8 MHz, which is in the radio frequency range (Bradley, 2000).

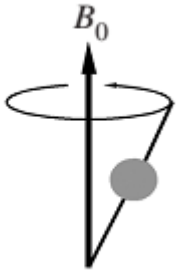

Figure 2.1: Precession of a proton around the field B_0 (Brown et al., 1998).

$$\omega_0 = \gamma . B_0 \qquad (2.1)$$

The human body mainly consists of water molecules which contain two hydrogen nuclei or protons. When the body lies in the magnetic field of the scanner, it becomes temporarily magnetized. This state is achieved when the hydrogen nuclei in the body align with the magnetic field's direction. When magnetized, the body responds to the exposure of the radiowaves at a particular frequency by sending back a radiowave signal called a "spin-echo". This phenomenon (NMR) only occurs at one frequency (the "Larmor frequency") corresponding to the specific strength of the magnetic field. The spin-echo signal is composed of multiple frequencies, reflecting different positions along the magnetic field gradient. When the signal is broken into its component frequencies (by a technique called a "Fourier Transform"), the magnitude of the signal at each frequency is proportional to the hydrogen density at that location, thus allowing an image to be constructed. Therefore, spatial information in MRI is contained in the frequency of the signal, unlike X-ray-based imaging modalities, such as CT (Bradley, 2000).

Diseased tissues, such as tumours can be disclosed due to the protons in different tissues where they return to their equilibrium stated at different rates. By changing the parameters on the scanner, this effect is used to create contrasts between different types of body tissues.

2.1.1(b) **The Radiofrequency Field**

The radiofrequency pulse is applied in the form of a small magnetic field provided by a coil placed in the *xy* plane. When placed, the sample inside the coil is subjected to both the static and oscillating fields. The oscillating field can be described by Equation 2.2.

$$B_{osc} = i2B_1 \cos\ (w_c t) \qquad (2.2)$$

Where B_{osc} is the oscillating field, i is the unit vector along the *x* axis, and B_1 is the variable magnetic field create from the coil, w_c angular velocities and t is the time.

When the magnetization has been tipped by the radio frequency pulse, the pulse is switched off and the magnetization will precess freely, decaying through the processes of relaxation back to the equilibrium value. The precession of the decaying magnetization induces a radio frequency voltage in the surrounding coil at the Larmor frequency, which is the source of the NMR signal. The degree to which the magnetization is tipped influences the strength of the signal induced in the coil since the largest signal will occur when the magnetization is precessing perpendicular to the coil in the *xy* plane. A pulse of duration τ_p that tips the magnetization onto the *xy* plane is called a 90^o or $\pi/2$ pulse, and one that inverts the magnetization along the z-axis a 180^o or π pulse (Cox, 2008).

2.1.2 **Relaxation Theory**

When a RF pulse is applied to a sample, the bulk magnetization may be mutated into the *xy* plane and induce a MR signal in a receiver coil positioned perpendicular to the *xy* plane. When the radiowave is switched off, the signal decays away. This decay is the result of the return of protons to the state that existed before the radio wave was applied. This return is termed as the Relaxation Time of the

protons. There are two mechanisms that cause the net magnetization to return to its equilibrium value: longitudinal (spin-lattice) relaxation and transverse (spin-spin) relaxation. Both processes account for the observed decay of the MR signal (Brown et al., 1998).

2.1.2(a) **Longitudinal Relaxation T1**

When a sample is placed in a magnetic field or after being subjected to a radiofrequency pulse on resonance, the nuclei reorient themselves so that the magnetization M_z tends to M_0. The return of magnetization in the longitude direction, z-axis (after a 90◦ pulse) is called spin-lattice longitudinal- or T1 relaxation. Spin-lattice relaxation is the loss of energy from the spinning nuclei to the surroundings (lattice). This relaxation is characterized by the time constant, T1 (Brown et al., 1998).

T1 is defined as the time between a complete 90◦ pulse and the relaxation which returns to 63 % of its original value as shown in Figure 2.2. This means that protons with different surroundings will relax with different T1 times and give a contrast between different compositions. T1 has a great dependency on the magnetic field's strength (Hendee and Ritenour, 2003; Hashemi et al., 2012). The reappearance of the axial magnetization follows an exponential relationship with the conventional characteristic time constant as described in Equation 2.3.

$$M_z(t) = M_0\left(1 - e^{-\frac{t}{T1}}\right) \tag{2.3}$$

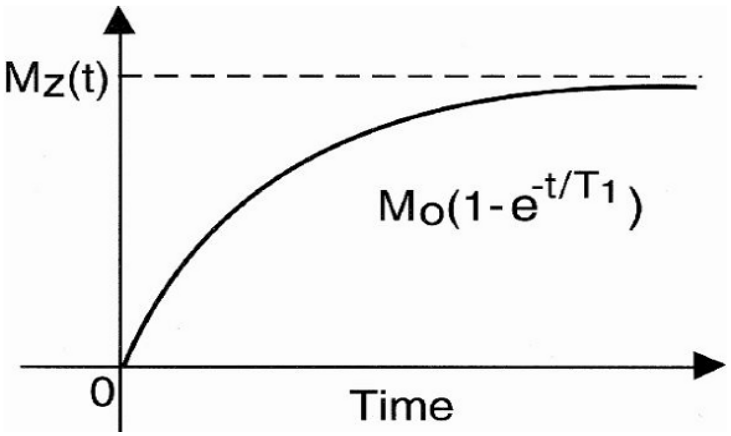

Figure 2.2: The graph of recovery of longitudinal magnetization with the growth rate of T1 (Hashemi et al., 2012).

2.1.2(b) **Transverse Relaxation T2**

The return of the transverse magnetization is called spin-spin transverse or T2 relaxation. The name spin-spin comes from the exchange of energy between the nuclei. Spin-spin relaxation is the loss of phase coherence in them due to the inhomogeneity of the magnetic field. The transverse magnetization, M_{XY} (t), at a time t after a 90° RF pulse is described by the Equation 2.4:

$$M_{XY} = M_0 \, e^{-t/T2} \qquad (2.4)$$

Where M_{XY} is the transverse magnetization immediately after a 90° pulse at t = 0, M_0 is the initial net magnetization. The magnitude of measured transverse magnetization is observed to have an exponential rate of decrease as shown in Figure 2.3 where as noted, T2 is defined as the time needed to decrease the original signal's strength to 37% (Hendee and Ritenour, 2003),

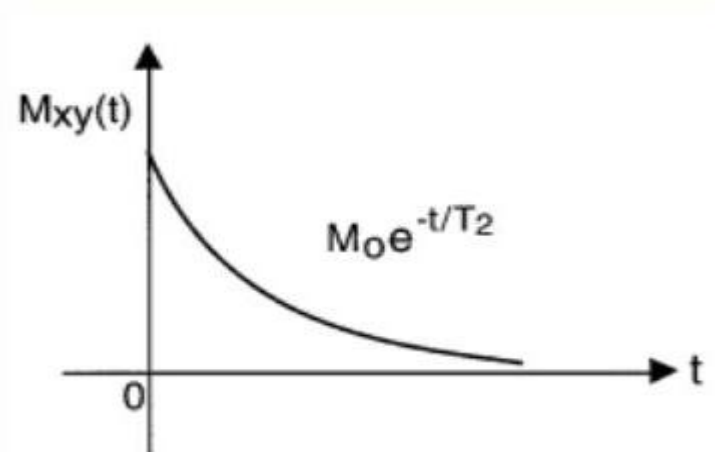

Figure 2.3: The graph of recovery of transverse magnetization with the decay rate of T2. (Hashemi et al., 2012)

For a given tissue, T2 is always shorter than T1 because the rate at which transverse magnetization decreases is faster than the rate at which longitudinal magnetization recovers along M_0. Biological materials may be characterized to some degree by their T1 and T2 values. T1 and T2 are greater in water than in solid materials (Blink, 2004).

2.1.3 **MRI Image Type**

The MR images can be acquired with several different techniques (pulse sequences) and acquisition parameters (called e.g. echo time, TE, repetition time TR etc.) resulting in different image contrasts. The image types mentioned below belong to the most commonly used MR.

2.1.3(a) **T1 Weighted image**

The T1 weighted scan uses a spin-echo (SE) or a gradient echo (GRE) sequence, the basic pulse sequences in MRI, and demonstrates differences in the T1 relaxation times of tissues. It is also used to differentiate anatomical structures mainly on the basis of T1 values; i.e. the scanning parameters are set (short TR/short TE) to minimize T2 relaxation effects. Tissues with high fat content (e.g. white matter) appear bright and compartments filled with water (e.g. Cerebrospinal fluid CSF) appear dark. This is good for demonstrating anatomy (Blink, 2004; Hendrick, 2007).

2.1.3(b) **T2 weighted image**

The T2 weighted image uses a spin-echo (SE) sequence or fast spin-echo (FSE).The scanning parameters are set (long TR/long TE) to minimize T1 relaxation effects. Compartments filled with water (e.g. CSF compartments) appear bright and tissues with high fat content (e.g. white matter) appear dark. This is good for demonstrating pathology since most (not all) lesions are associated with an increase in water content. T2 is always shorter than T1 (Hendrick, 2007).

2.1.4 **MRI contrast**

Contrast is the differences in signal intensity between surrounding tissues. The normal contrast in MRI depends on the proton spin density and relaxation times, (T1, T2) (Hendee and Ritenour, 2003). The MR image contrast can be controlled by changing the pulse sequence parameters. This involves the setting of a specific number, strength, and timing of the RF and gradient pulses. In the pulse sequences are the repetition time (TR) and the echo time (TE). The TR is the time between

successive 90˚RF pulses while TE is the time between the initial 90˚ degree RF pulse and the MR signal echo as shown in Figure 2.4.

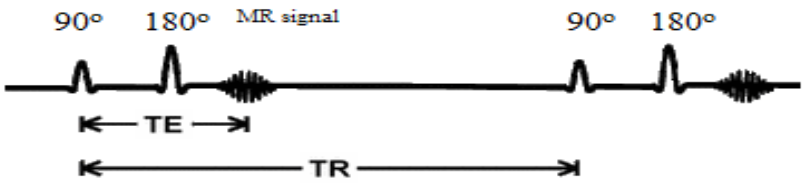

Figure 2.4: The spin-echo pulse sequence, schematic representation of TR and TE (Maravilla and Cohen, 1991).

The contrasting signals can be an altered or weighted image, e.g. if a long TE used the inherent differences in T2, all tissues will become apparent (water), take longer to decay, and their signals will be greater or appear brighter in the image compared to tissues with a short T2 (fat) which appear dark. Similarly, in T1 images, tissues with a long TR (water) will take a long time to recover back to their equilibrium point. Therefore, it will appear darker compared to tissues with short T1 (fat). Table 2.1 shows MRI signal intensities with T1, T2 weighted images. For most lesions, including breast cancers, they have the highest T1 and T2 values compared to normal tissues. The reason is that lesions tend to have higher water concentrations and therefore, fewer macromolecules per unit volume than normal tissues (Hesselink, 1996).

Table 2.1: MRI image appearance

Material	T1 weighted	T2 weighted
Water	Dark	Bright
Fat	Bright	Dark
Blood	Gray	Dark

2.1.5 **Brief Review of MRI**

Lauterbur in 1972 devised the term 'zeugmatography' for the joining of a magnetic field and spatially defined radiofrequency field gradients to generate a two-dimensional display of proton density and relaxation times in tissues. The first nuclear magnetic resonance image used various combinations of magnetic field gradients (Lauterbur and Foster, 1980).

The MRI has been applied to characterize wood since the late seventies to the early eighties and is an important technique to non-destructively image the gross structural features of wood as well as being able to map diffusion and monitor flow of moisture in wood (Wang and Chang, 1986; Merela et al., 2005). Wood can be characterized through the determination of parameters, such as chemical shift, moisture content distribution and water proton diffusion. This provides unique parameters such as the relaxation time of the water protons. Was used the C13 MR spectroscopy to follow the incorporation of CO_2 into sugars and lipids such as soy beans where in 1984, the water flow in an intact cucumber plant was measured by Van As and Schaafsma (1984). Later, Hall et al. (1986) used the magnetic resonance scanner to obtain images at 0.14 T based on the water in Aspen (*Populus Tremuloides Michx*) and to visualize the expected structural features such as annual growth-rings and knots. He discovered that wood does not contain sufficient water to give an image. Later on, Araujo et al. (1992) studied two new proton magnetic

resonance techniques, relaxation spectra and relaxation selective imaging used to investigate the distribution of water in samples of normal white spruce sapwood, heartwood, and juvenile wood, as well as two rehydrated heartwood samples containing incipient decay and compressed wood respectively. It is demonstrated that the spin-spin (T2) relaxation behavior in wood is best presented as a continuous spectrum of relaxation times. Water environments which are separable on a T2 spectrum may be imaged separately. They demonstrated that above the fiber saturation point, the moisture density profile of the bound water is largely independent of moisture content. The feasibility and utility of using these techniques for internal scanning of logs and lumber are discussed. These techniques should provide new insights into the wood drying process.

Herlihy et al. (2005) studied the Spruce wood blocks (1.5 x 1.5 x 3 cm), were completely saturated with water and allowed to dry under ambient conditions to achieve a 12% moisture content, using MRI scanner at 9.4 T Ultrashort TE (UTE) imaging techniques. In addition, oil phantom was placed on top of the wood samples for the spin echo imaging to determine the position of the wood block. The results shown the wood is readily distinguished by UTE, thus providing a means to assess moisture content and preservative distributions between these woody tissues. The dry wood phantoms have the added benefit of providing a challenging imaging model with which to develop UTE imaging techniques.

Since the 1980s, MRI is used in body composition studies as it is a noninvasive diagnostic tool that provides anatomical, physiological and soft tissue image, (Foster et al., 1984; Nair et al., 2010). The methods are based on the fact that the relaxation times are different in tissues. Clinically, the MRI methods based on

relaxation times are rarely used due to the very long acquisition time required to obtain accurate T1 and T2 maps of the tissue.

Merchant et al. (1993) studied the T1 and T2 relaxation times that were determined for normal breast tissues along with malignant and benign breast tumors from pure T1 and T2 images calculated using the mixed sequence data spin-echo (SE) inversion-recovery (IR) imaging sequence. The results showed that the T1 value in benign tumors of (1049.02 ms ± 40.31) is bigger than that of malignant tumors (876.09 ms ± 27.83). In addition, normal tissues (795.64 ms ± 21.12) values for T2 in benign tumors (89.15 ± 8.33) are also bigger than the mean value of normal tissues (62.82 ms ± 4.06).

In 1999, the concentrations and proton relaxation times of major metabolites in the human hippocampus were studied (Choi and Frahm, 1999). Later on, relaxation time was measured for the human brain at 3 T. The results showed the T1 relaxation times obtained ranging from 0.97 to 1.47 ms for grey matter and from 0.87 to 1.35 ms for white matter. On the other hand, T2 relaxation times range from 116 to 247 ms and from 141 to 295 ms in grey and white matter respectively (Mlynárik et al., 2001).

In 2006, Rakow-Penner et al. (2006) measured the T1 and T2 of breast fibroglandular tissue and fat at 1.5 T and 3T where he noted the partial volume effects of the admixture of fibroglandular tissue and fat. The relaxation rates used an approach termed iterative decomposition of water and fat which was applied on the right breasts of five healthy women. They found that the T1 increased for both fat (21%) and glandular tissue (17%) from 1.5T to 3T and there was no significant difference between T2 values due to tissue types or field strength.

Keenan et al. (2016) was designed a breast phantom to enable quantitative assessment of 1.5 T and 3.0T MRI by measurements of T1 relaxation time and apparent diffusion coefficient (ADC), A breast phantom was fabricated with two independent, interchangeable units for diffusion and T1/T2 relaxation, and outer shells flexible, the unit was filled with corn syrup solution and grapeseed oil to mimic the relaxation behavior of fibroglandular and fatty tissues, respectively for T1 and plastic tubes filled with aqueous solutions of polyvinylpyrrolidone (PVP) to mimic the ADC. The results show the fibroglandular mimic exhibited target T1 values on 1.5T and 3.0T clinical systems and the PVP solutions mimicked the range of ADC values from malignant tumors to normal breast tissue, therefore, this phantom can be enables variety of clinical breast coils, and can serve as a quality control tool to facilitate the standardization of quantitative measurements for breast MRI.

In MRI principle work, relaxation times of the hydrogen proton are important (the longitudinal relaxation T1 and T2 transverse relaxation). The relaxation times are affected by the physical state of the proton or water molecule. This was studied by Cox (2008) who investigated the relaxation time (T1 and T2) of the wood and water components that are established using the standard one dimensional (1D) procedures and furthered by the application of the 2D of T1-T2 correlation experiment.

The relaxation times are important in this thesis as for the first time this study focuses on investigating the relaxation time in the *Rhizophora* spp. wood, which is equivalent to human tissues in two parts, fresh wood and particleboard.